Available online at www.sciencedirect.com
ScienceDirect
Earth and Planetary Science Letters 265 (2008) 96–111
EPSL
www.elsevier.com/locate/epsl

Discontinuous and diachronous evolution of the Main Ethiopian Rift: Implications for development of continental rifts

K. Keranen *, S.L. Klemperer

Department of Geophysics, Stanford University, 397 Panama Mall, Stanford, CA USA

Received 26 March 2007; received in revised form 14 September 2007; accepted 25 September 2007
Available online 6 October 2007
Editor: C.P. Jaupart

Abstract

The Main Ethiopian Rift (MER) is commonly considered the archetypal magma-assisted rift. Tomographic images of upper-mantle upwellings beneath the rift, aligned anisotropy beneath magmatic segments, and pervasive magmatic modification of the crust all indicate the importance of magmatic processes in present-day rift evolution. It has been suggested that this magmatic development is responsible for the straight and continuous path the rift cuts across the Ethiopian Plateau. We compile new evidence indicating that the MER is not as continuous and its development not as simple as previously believed. Significant lithospheric heterogeneities are evident in our compilation of recently acquired seismic, gravity, and geologic data. Numerical models of rift propagation in such heterogeneous lithosphere show that rift propagation may stall at rheological boundaries. We propose that the heterogeneities in the MER caused irregular rift propagation, resulting in a distinct discontinuity visible within the rift lithosphere. This discontinuity in structure spatially correlates to an apparent discontinuity in the age of extension between the northern MER and the central MER, lending support to our hypothesis.

Our interpretation leads to a two-phase model of rift propagation in the MER, with initial rift development primarily controlled by lithospheric structure and a later phase during which magmatic processes are dominant. During the initial phase, rift propagation was irregular and at times stalled or was diverted away from the modern rift trend along pre-existing structures. Our model, while acknowledging the importance of magmatic processes in volcanic extensional regions, shows that even in this classic example of magma-assisted rifting, inherited lithospheric structure localized initial extension and controlled rift propagation. This early phase formed the template for future rift development and continental break-up.

Keywords: Ethiopia; Main Ethiopian Rift; lithosphere; extension; rift propagation

1. Introduction

The Main Ethiopian Rift (MER) provides a unique natural environment to observe the initiation and evolution of rifting in a heterogeneous Precambrian craton modified by Tertiary plume magmatism. It is commonly suggested that rift propagation in the MER progressed northward (e.g. Keir et al., 2006; Mackenzie et al., 2005; Wolfenden et al., 2004), although the evolution is not well understood. Alternative hypotheses, such as a proposed model of rift initiation via dike emplacement from beneath Afar (Buck, 2006) or a model of northward plate motion over a stationary hotspot

* Corresponding author. Tel.: +1 650 724 0461; fax: +1 650 725 7344.
E-mail addresses: kkeranen@stanford.edu (K. Keranen), sklemp@stanford.edu (S.L. Klemperer).

0012-821X/$ - see front matter © 2007 Elsevier B.V. All rights reserved.
doi:10.1016/j.epsl.2007.09.038

(Rogers, 2006), imply southward propagation. Models of active rifting above mantle upwellings (small-scale convection in the upper mantle; Kendall et al., 2006) imply little to no propagation along-axis. Bonini et al. (2005) suggest a heterogeneous time-space propagation, with initial extension in the Southern Main Ethiopian Rift (SMER) propagating northward until 11 Ma, southward propagation of the Northern Main Ethiopian Rift (NMER) from Afar after 11 Ma, and formation of the Central Main Ethiopian Rift (CMER) since 5–6 Ma. Most of these previous models have been developed based on surface geologic data (Bonini et al., 2005; Wolfenden et al., 2004) or on conceptual models of the rifting process (Buck, 2006; Rogers, 2006) with little regard to the lithospheric structure.

However, observations of many continental rifts show that they preferentially follow pre-existing weaknesses in continental lithosphere and branch around stronger cratons (Dunbar and Sawyer, 1988; Nyblade and Brazier, 2002; Tommasi and Vauchez, 2001; van Wijk, 2005). Suggested causes of weakness include orogenic belts, rheological heterogeneities (Dunbar and Sawyer, 1989), mechanical anisotropy of the mantle (Vauchez et al., 1997,1998), thermal disturbances (Hill, 1991), and base-lithosphere pre-existing topography (Ebinger and Sleep, 1998; Pascal et al., 2002). The locations of rifts appear to be primarily controlled by these inherited structures. The dynamics of rift propagation in such heterogeneous lithosphere have been modeled by numerous authors (Courtillot, 1982; Courtillot and Vink, 1983; Dunbar and Sawyer, 1989, 1996; Sawyer, 1985; van Wijk and Blackman, 2005). These studies model an initial weakness within the crust or lithosphere to represent a pre-existing weak zone. Without such a weak zone, models predict that extension is widely distributed. Dunbar and Sawyer (1996) and van Wijk and Blackman (2005) model a lithospheric weakness extending across only part of the model, initially localizing extension in the weak zone. The locked zone undergoes diffuse extension until the rift tip arrives. At this point, focused extension may propagate across the discontinuity or may stall for millions of years (van Wijk and Blackman, 2005). The zone of focused extension that develops across the boundary may be offset from the prior zone of extension.

Geophysical observations in the MER can be used to map lithospheric properties and spatial variations in extension and magmatism, and provide a critical third dimension to constrain models of rift evolution. These observations provide insight not only into the inherited structures which control rift evolution, but also into spatial variations in extension and magmatism which result from irregularities in rift evolution and therefore serve as markers of the extensional process. We present a three-dimensional model of heterogeneous lithospheric structure in the Main Ethiopian Rift based on our compilation of recent geophysical and geological data, and use this model together with the most recent geochronologic information to relate rift development and propagation to inherited structures. We conclude that the sectorization seen at the surface is fundamental, extends through the crust into the upper mantle, and reflects the nature of the processes that have created the rift. We interpret the Yerer-Tullu Wellel Volcanotectonic Lineament (YTVL), which has traditionally been considered distinct from the Cenozoic rift system, as an integral part of the Main Ethiopian Rift evolution.

2. Tectonic setting

The Main Ethiopian Rift is a seismically and volcanically active portion of the East African Rift System (EARS) trending NE across the Ethiopian plateau (Fig. 1). The MER developed within the Mozambique Belt, a broad Proterozoic mobile belt which extends from Ethiopia south through Kenya, Tanzania and Mozambique. The Mozambique Belt is believed to represent a Himalayan-type continental collision zone (Burke and Sengor, 1986; Shackleton, 1986), and ophiolites mark numerous sutures within the basement complex of Ethiopia (Berhe, 1990; Stern et al., 1990; Vail, 1985) although the trend of the sutures is contentious (Church, 1991). The suture is also evident in neodymium (Nd) isotopic data (Stern, 2002), which indicates a major crustal boundary in Ethiopia separating juvenile crust in the north and west (mean age 0.87 Ga) from reworked Paleoproterozoic and Archean crust (mean age 2.0 Ga) to the east (Stern, 2002).

Flood basalts erupted primarily between 31–29 Ma cover much of the Proterozoic basement, extending over an area of the Ethiopian plateau ~1000 km in diameter (Baker et al., 1996; Hofmann et al., 1997; Ukstins et al., 2002). A mantle slow-velocity anomaly underlies the rift (Bastow et al., 2005; Benoit et al., 2006; Montelli et al., 2006) down to at least 650 km depth beneath Afar and rising to at least 75 km depth beneath the Main Ethiopian Rift. The shallow part of this anomaly is offset ~25 km from the rift axis (Bastow et al., 2005) and dips westward, possibly connecting to the African Superplume (Benoit et al., 2006) although direct evidence remains elusive.

The MER has traditionally been divided into three sectors based on surface geology and geomorphology,

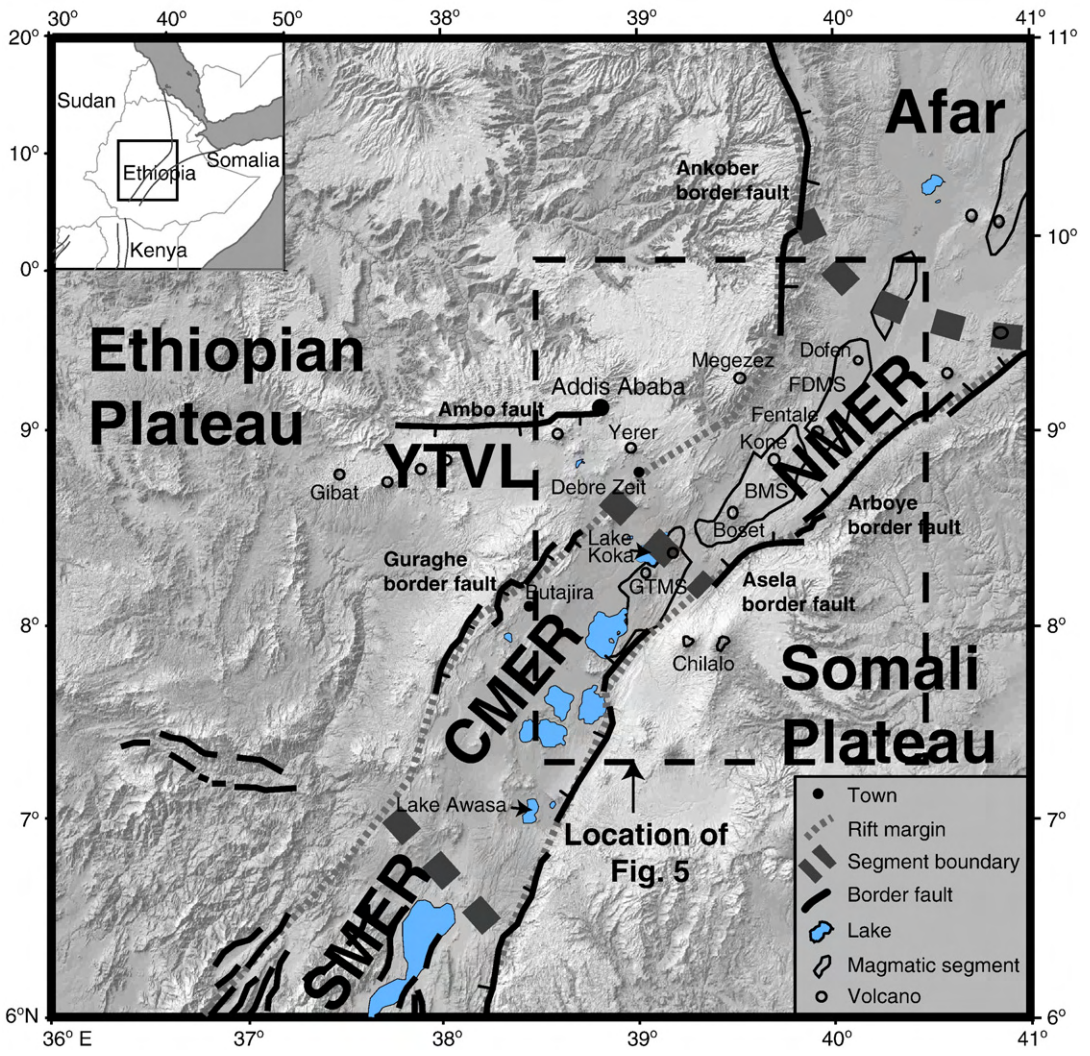

Fig. 1. Location of the Main Ethiopian Rift. Main rift segments are the Northern Main Ethiopian Rift (NMER), the Central Main Ethiopian Rift (CMER), and the Southern Main Ethiopian Rift (SMER). The Yerer–Tullu Wellel Volcanotectonic Lineament (YTVL) trends ~E–W from the southern end of the NMER between ~8° and 9°N. Thick dashed gray lines represent sector boundaries between the NMER, CMER, and SMER (Ebinger and Hayward, 1996). Thin dashed gray lines represent approximate MER boundaries. FDMS: Fentale–Dofen Magmatic Segment, BMS: Boset Magmatic Segment, GTMS: Gademsa–Tullu Moye Magmatic Segment. Dashed box shows the location of Fig. 5.

the northern (NMER), central (CMER), and southern (SMER) sectors (Fig. 1). The NMER extends south from the Afar depression to near Lake Koka, with border faults that trend on average at N50°E and have formed since 10–11 Ma. Early volcanism also began at 10–11 Ma (Chernet et al., 1998; Wolfenden et al., 2004). The CMER extends from Lake Koka through the lakes region to Lake Awasa, with border faults trending on average N30°E–N35°E. The age of onset of extension in the CMER is still debated. WoldeGabriel et al. (1990) estimate the age of onset of faulting to be 8.3–9.7 Ma with earliest synrift volcanics at ~8 Ma, whereas Bonini et al. (2005) estimate the onset of extension and initial volcanism to be 5–6 Ma. The SMER extends south from Lake Awasa into the broadly rifted zone of southern Ethiopia (Ebinger et al., 2000) with faults trending north–south to N20°E. Faulting in the SMER was well-established by ~18 Ma (Ebinger et al., 1993; Wolde-Gabriel et al., 1991), and volcanism began around 18–21 Ma (Ebinger et al., 1993; George and Rogers, 2002).

Within these larger sectors, the MER is composed of rift segments bounded by steep border faults ~50 km long (Fig. 1) with greater than 3 km throw. Active deformation within the NMER is concentrated in ~20-km-wide magmatic segments consisting of rift volcanoes, basaltic fissures, and young fault belts, with a

north-northeast trend oblique to the overall rift trend. Seismicity in the NMER as recorded in a 16-month deployment (Fig. 2) occurs in these magmatic segments and also along the rift-boundary faults, while seismicity in the CMER during the same time period was localized only near the eastern rift margin (Keir et al., 2006). Quaternary volcanism has occurred in the magmatic segments beginning ca. 1.6 Ma, near Butajira and Debre Zeit along the western rift margin in the CMER, along the Yerer–Tullu Wellel Volcanotectonic Lineament (YTVL; Abebe et al., 1998), and at Chilalo volcano on the southeast rift shoulder (Fig. 1). Poisson's ratio values inside the rift valley greater than 0.32 (Dugda et al., 2005; Stuart et al., 2006), historical flows at Fentale in 1820 (Gibson, 1969) and elevated temperatures in geothermal wells near Aluto (Endeshaw, 1988) are strongly suggestive of ongoing magmatism.

The YTVL (Fig. 1) is a trend of volcanoes and fracture systems trending roughly east-west between ~8.5–9 N, intersecting the MER at the NMER–CMER boundary. This zone is not commonly thought of as part of the Cenozoic rift system. An east-west trending border fault bounds the northern border of the YTVL (the Ambo fault) and offsets the flood basalts vertically by ~500 m. Volcanoes in the YTVL were active coevally with volcanoes along the eastern margin of the NMER (Chernet et al., 1998), and extension along the Ambo fault began at the same time as extension in the

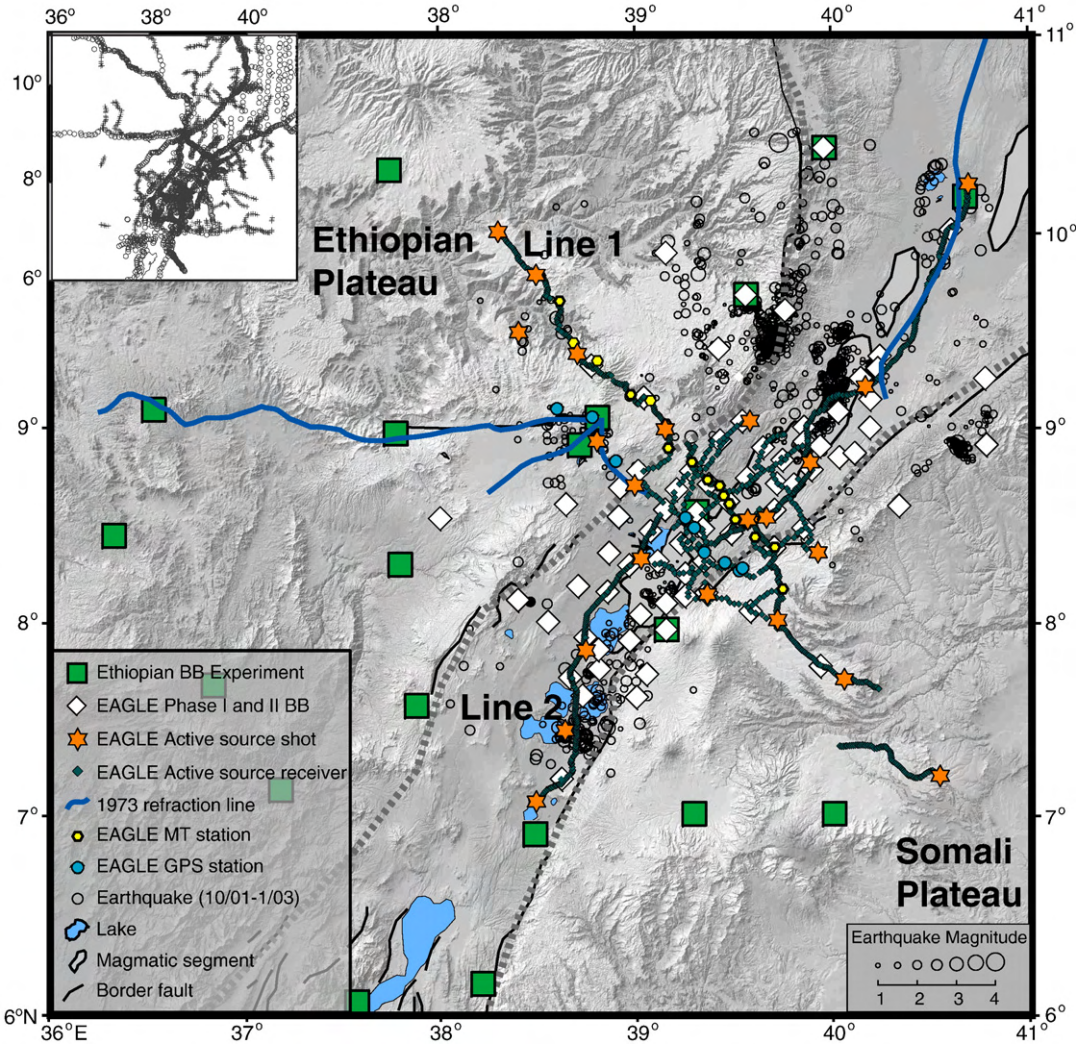

Fig. 2. Locations of geophysical data collected during EAGLE (Maguire et al., 2003), the Ethiopian Broadband (BB) Experiment (Nyblade and Langston, 2002), and by a 1973 refraction survey (Berckhemer et al., 1975). Broadband and gravity stations (neither shown) were also located along the controlled-source across-axis line (Line 1) at ~5-km intervals. Earthquake locations are from Keir et al. (2006). Gravity stations (Ebinger and Hayward, 1996) are shown in the inset, which covers the same area as the main figure. Rift boundaries and border faults from Fig. 1.

NMER. A low-velocity anomaly visible in the upper mantle tomography (Bastow et al., 2005) follows the NMER and then deflects to the west beneath the YTVL. No border fault is present along the western boundary of the MER which instead forms a gentle monocline where the rift system intersects the YTVL.

3. Constraints on the timing of extension and magmatism in the MER and YTVL

Numerous authors have contributed to the understanding of the timing of volcanism and extension in the MER (e.g. Bonini et al., 2005; Wolfenden et al., 2004; and references therein). Magmatic activity in the MER has been episodic rather than continuous. Volcanism began with flood basalts over a broad area of the Ethiopian and Somalia Plateaus, with the greatest eruption rates from 31–29 Ma (Baker et al., 1996; Hofmann et al., 1997; Ukstins et al., 2002). These trap basalts lie unconformably on Mesozoic sediments and are found in both the NMER and the CMER (Bonini et al., 2005; Wolfenden et al., 2004). A second phase of flood basalt volcanism in the NMER and the CMER occurred at 10–11 Ma (Chernet et al., 1998; Wolfenden et al., 2004). Time-correlative basaltic units are widespread on both plateaus. In both the CMER and the NMER, a period of felsic volcanism occurred between 3.5 to 2.5 Ma (Wolfenden et al., 2004). Since 1.8 Ma, bimodal volcanism has been largely correlated with the Wonji fault belt (Bonini et al., 2005; Wolfenden et al., 2004).

3.1. Onset of extension in the CMER

The timing of the main phases of extension in the CMER and in the NMER has been studied by Bonini et al. (2005) and Wolfenden et al. (2004) respectively. Bonini et al. focused on the Guraghe margin in the CMER (Fig. 1), which has a well-exposed succession spanning from the Oligocene to the Late Pliocene. The oldest rocks are basaltic, and dated at 29 Ma (Bonini et al., 2005). The authors link these rocks to the initial phase of flood basalts covering a wide region of Ethiopia. Above this unit is an unconformity, with an extended period of non-deposition until 10.25–8.4 Ma. Starting at ~10.25 Ma the Guraghe–Anchar basalts were deposited at the Guraghe margin. These basalts are also found on the western rift plateau 75 km from the rift and on the eastern rift margin. This wide distribution implies a thin but extensive flood basalt sequence at 11.5–8 Ma over a low-relief landscape in the CMER (Bonini et al., 2005). These flows show no evidence of growth. The final episode of volcanism at the top of the Guraghe succession provides evidence for the onset of extension. The unit consists of 5 to 3 Ma basalts, correlative with the Nazret Unit found throughout the CMER, and shows syn-rift growth (Abebe et al., 2005). Based on the architecture of this unit, Bonini et al. (2005) interpret the beginning of the main rifting phase in the CMER at the Miocene-Pliocene boundary, with most tectonic activity occurring after 5 Ma.

3.2. Onset of extension in the NMER

Wolfenden et al. (2004) studied a cross-section across the Adama basin in the NMER (Fig. 1), from the Ankober border fault and Megezez volcano in the NW to the Arboye border fault system in the SE. On the deeply incised flanks of the Adama basin, Ar/Ar and K/Ar dating show 26 to 23.4 Ma flood basalts overlying Mesozoic sediments. A hiatus in volcanism then occurred until ~10.5 Ma (Chernet et al., 1998; Wolfenden et al., 2004), corresponding to the hiatus also present in the CMER. At ~10.5 Ma, plateau basalts from Megezez volcano were deposited and are onlapped by basalts from the Kessem formation, which was deposited beginning at 10.6±0.05 Ma (Wolfenden et al., 2004). The Kessem basalts show growth and syn-sedimentary faulting, and faults that terminate within or at the top of the Kessem formation are sub-parallel to the Arboye border fault (Wolfenden et al., 2004). These data indicate that the Arboye border fault system developed at ~10.6 Ma and controlled basin geometry (Wolfenden et al., 2004). Wolfenden et al. (2004) argue that the conformable contact between the Megezez flows/Kessem formation and the flood basalt sequences indicates no significant deformation in the northern MER prior to 10.6 Ma. Silicic centers of the Gara Gumbi trachytes along the southeastern margin of the NMER developed from 7 to 5 Ma (Chernet et al., 1998).

3.3. Volcanism and extension in the YTVL

The timing of extension and magmatism in the YTVL was presented by Abebe et al. (1998). The YTVL has a similar volcanic succession to the MER, with Mesozoic sedimentary rocks overlain by flood basalts from the initial sequence between 33 and 28 Ma. These flood basalts are followed by a hiatus until ~12 Ma, after which time they were overlain by Late Miocene to Recent basalts and silicic volcanoes. The early flood basalts are downthrown ~500 m across the Ambo fault, the bounding fault on the northern edge of the YTVL. A histogram of age distribution in the YTVL shows a remarkably similar character to that of the NMER, with a period of eruption

from 11 to 7 Ma, from 6 to 3.5 Ma, and younger than 1 Ma (Abebe et al., 1998). Chernet et al. (1998) link the silicic volcanoes of the Gara Gumbi group in the NMER to the silicic volcanoes in the YTVL, which also developed from ~7 to 5 Ma. Based on the relationship of the volcanic activity to the structures in the YTVL, Abebe et al. (1998) consider the onset of the 12 Ma volcanic sequence to reflect the beginning of the tectonic movements responsible for the formation of the YTVL.

4. Geophysical data

The amount of data available in the Main Ethiopian Rift has increased significantly in recent years (Fig. 2). Along with recent geological studies (Abebe et al., 2007; Bonini et al., 2005; Pizzi et al., 2006; Wolfenden et al., 2004) and the Ethiopian Broadband Experiment (Benoit et al., 2006; Dugda et al., 2005; Nyblade and Langston, 2002), the 2001–2003 EAGLE (Ethiopia-Afar Geoscientific Lithospheric Experiment) project (Maguire et al., 2003) deployed the largest number of seismic instruments to date on the African continent and collected new seismic (Bastow et al., 2005; Maguire et al., 2006; Stuart et al., 2006), gravity (Cornwell et al., 2006; Mickus et al., 2007), seismicity (Keir et al., 2006), geodetic (Bendick et al., 2006), magnetotelluric (Whaler and Hautot, 2006), and geochemical data (Furman et al., 2006, Rooney et al., 2005, in press).

Our 2003 controlled-source seismic experiment within the EAGLE project recorded data on ~400 km refraction lines along and across the rift (Mackenzie et al., 2005; Maguire et al., 2006) (Fig. 3) and an ~100-km-diameter two-dimensional array spanning the rift (Fig. 2; Keranen et al., 2004). EAGLE passive source seismic data were collected from 170 stations centered on the Boset magmatic segment covering a region 250×350 km within the NMER and its flanks (Fig. 2). Three phases of broadband seismometers were deployed (Maguire et al., 2003), with average station spacings of ~40 km (29 stations spanning the rift and rift shoulders), ~15 km (50 stations within the rift), and ~5 km (91 stations in a linear array within the across-rift active source line). The Ethiopian Broadband Experiment (Nyblade and Langston, 2002) collected data at 27 sites from 2000–2002, spread over a broad region with 22 sites on the eastern and western plateaus and 5 stations inside the MER or in the Afar depression. EAGLE gravity data were collected at 300 sites distributed along two lines along the axis of the rift at 1-km spacings (Fig. 2) (Mickus et al., 2007) and at 72 sites with ~5 km spacing along the across-axis line (Cornwell et al., 2006), and merged with data collected by the Geological Survey of Ethiopia and a compilation of open-source data (Ebinger and Hayward, 1996).

5. Lithospheric properties of the Ethiopian and Somali Plateaus

It is evident from observations and numerical models that inherited structure can control the location of rifting, and possibly also the style of rifting. Based on our compilation of geophysical data, we interpret three distinct pre-existing lithospheric domains around the Main Ethiopian Rift which we interpret below to have controlled the location and the continuity of the extensional process. The western shoulder, or the Ethiopian Plateau, has a strong north–south decrease in crustal thickness allowing division into northwestern and southwestern blocks at the YTVL. The third domain is the eastern shoulder, the Somali Plateau.

The northwestern block has the strongest heterogeneities at its boundaries, and appears to have had the strongest influence on the development of the MER. In this block, a high-velocity 7.4 km/s layer beneath the northwestern shoulder (Mackenzie et al., 2005) creates a 40–50 km thick crustal block (from data in Berckhemer et al., 1975; Dugda et al., 2005; Mackenzie et al., 2005; Stuart et al., 2006) with a mafic root, and strong crustal property variations, hence rheological boundaries, along its eastern edge (the NMER) and along its southern edge (the YTVL) (Fig. 4). Across the YTVL, the western shoulder thins rapidly from >40 km thick to 34–36 km thick (Berckhemer et al., 1975; Dugda et al., 2005; Stuart et al., 2006). The third block, the eastern shoulder, is of relatively constant thickness from north to south and has no 7×km/s layer.

The high-velocity layer beneath the northwestern shoulder is interpreted to be underplated mafic material emplaced in association with the voluminous flood basalts at 30 Ma (Mackenzie et al., 2005), accumulated beneath ~35 km thick crust (based on the thickness of the normal crust above the underplate and the thickness of the adjacent unmodified crust to the south) as compared to 38–40 km thick crust beneath the eastern shoulder (Dugda et al., 2005; Mackenzie et al., 2005; Stuart et al., 2006). We interpret that the Precambrian crust of the western shoulder is the same from north to south, with Oligocene underplating beneath only the northern section creating the two separate provinces. It is unlikely that distributed extension across the southwestern shoulder, if present prior to the onset of extension in the CMER, would have been enough to decrease its thickness from 40 to 35 km if it had also originally been underplated, and therefore the SW shoulder represents the original crustal thickness for the western province.

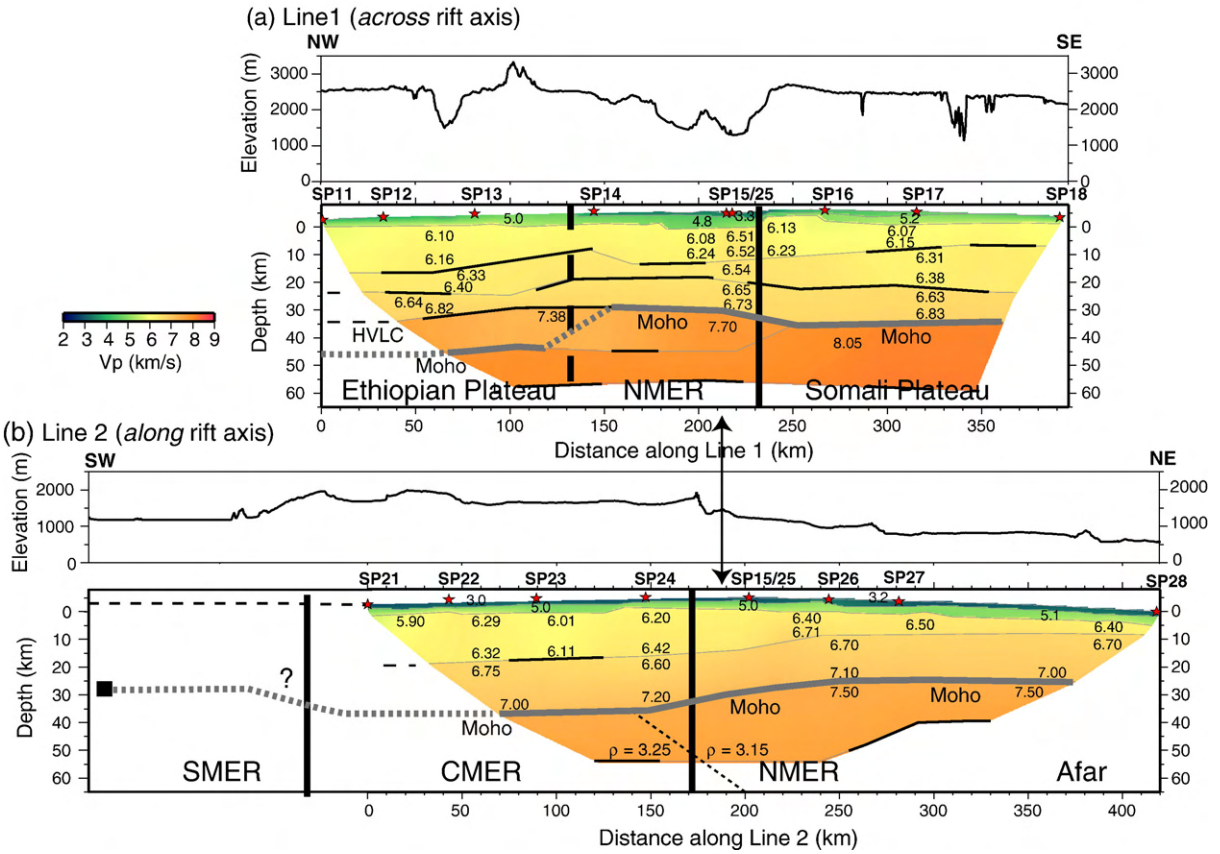

Fig. 3. Cross-sections across (a) and along (b) the rift axis from the EAGLE controlled-source experiment, modified from Maguire et al. (2006). (a) Velocity model of Line 1, across the rift axis (Mackenzie et al., 2005). P-wave velocities are given in km/s. (b) Velocity model of Line 2, along the rift axis (Maguire et al., 2006). Line 2 has been extended in the south to include the SMER, constrained by a receiver function from the Ethiopian Broadband Seismic Experiment (Dugda et al., 2005). The vertical axis and horizontal offsets are in a local Cartesian coordinate system defined for the project area. The curvature of the earth appears as a topographic bulge in the model, i.e. increasing the apparent elevation of the shots (red stars) in the center of the project area. The superjacent elevation profiles are plotted with respect to sea level. HVLC — high velocity lower crust; solid black lines — reflectors; vertical lines — segment boundaries (dashed at the poorly localized monoclinal boundary between the Ethiopian Plateau and the NMER); solid gray line — Moho; dashed gray line — approximate location of Moho. The dashed black line in (b) shows the boundary between an upper mantle with density of 3.25 kg/m^3 and 3.15 kg/m^3 from the model of Mickus et al. (2007).

We interpret that the inherited lithospheric structure was the primary controlling factor on the development of the MER, as evidenced by observations of lithospheric property variation, hence variable extension and magmatism, within the MER itself.

6. Lithospheric properties of the NMER, CMER and YTVL

6.1. Overview

Crustal thickness and velocity structure, in combination with related geological and geophysical data, can be used to characterize spatial variability in extension and magmatism. These spatial patterns allow us to evaluate the continuity of extensional processes and relate this to the nature of rift propagation and inherited lithospheric structure.

Crustal structure is constrained by controlled-source seismic data (thickness and velocity), receiver function estimates of crustal thickness and Poisson's ratio, and gravity models (Figs. 3–6). Existing data are unevenly distributed and each sector has a different type and/or degree of constraint. The data available are concentrated in the NMER and the CMER, and with our analysis we redefine the boundary between these two sectors.

6.2. Structure of the NMER and CMER — extension and magmatism

The NMER is well-characterized by seismic and gravity data. This rift sector has thin crust relative to the

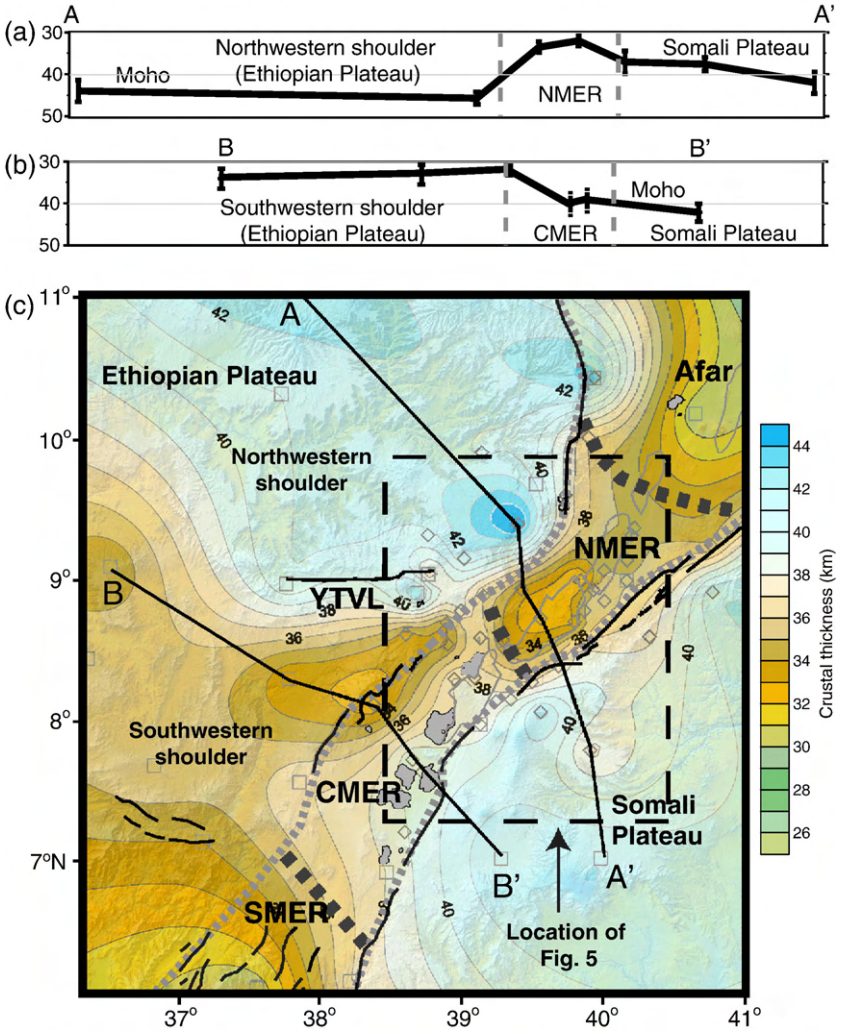

Fig. 4. Profiles of cross-sections (a) A–A' and (b) B–B' and (c) contour map of crustal thickness. Data are from the Ethiopian Broadband Network (Dugda et al., 2005) and from EAGLE Phase I and Phase II stations (Stuart et al., 2006). Data from the EAGLE controlled-source survey (Fig. 3) were not included so that Figs. 3 and 4 represent entirely independent observations of crustal thickness changes across province and segment boundaries. Note cross-section A–A' is clearly similar to the Moho profile in Fig. 3a. Note the relative thickness difference between the NMER and the CMER. Rift outlines are as in Fig. 1, but the boundary between the NMER and the CMER has been redefined based on our interpretation (see text).

CMER and to the rift shoulders. The crust is thickest in the south, 33–35 km thick adjacent to the CMER, and gradually thins to the north along the rift axis to ~26 km in southern Afar (Maguire et al., 2006; Mickus et al., 2007; Stuart et al., 2006) (Fig. 3). The majority of this thinning occurs in the upper crust, which also has high upper-crustal velocities of 6.4–6.7 km/s (Keranen et al., 2004, Mackenzie et al., 2005). P_n velocities measured at 7.5 km/s are below the global average.

A cross-section across the NMER shows a typical crustal thickness profile for a rift (Figs. 3a and 4a), with large border faults bounding the rift, and rift shoulders that are 5–15 km thicker than the crust beneath the rift valley. This rift sector includes well-developed magmatic segments, with faults, fissures, and active eruptive centers (Fig. 1). The high velocity in the upper crust reaches a maximum beneath these magmatic segments, which have relative positive Bouguer anomalies (Cornwell et al., 2006; Keranen et al., 2004; Mahatsente et al., 1999; Tiberi et al., 2005), and are interpreted as amalgamated and mostly cooled gabbroic dike complexes (Keranen et al., 2004; Rooney et al., 2005). Beneath the Fentale–Dofen magmatic segment, a spatial correlation exists between the highest upper-crustal

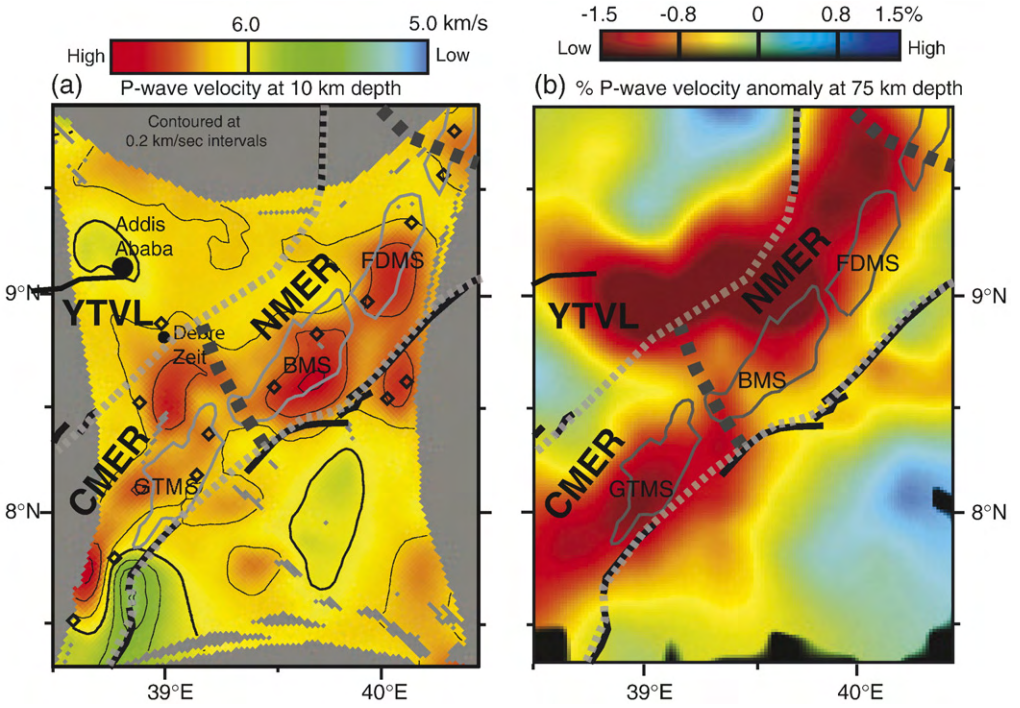

Fig. 5. Depth slices from (a) controlled-source tomography at 10 km below the rift valley floor (modified from Keranen et al., 2004); and (b) passive-source upper mantle P-wave tomography at 75 km depth (modified from Bastow et al., 2005). The high-Vp (red) bodies in (a) are interpreted as magmatic intrusions and the low-Vp (red) bodies in (b) as reflecting partial melt and higher upper mantle temperature. Border faults are shown as black lines; magmatic segments are outlined in thin gray lines; locations of rift-valley volcanoes shown by black diamonds. Rift outlines and segment boundaries from Fig. 1 with our updated NMER–CMER boundary. FDMS: Fentale–Dofen Magmatic Segment, BMS: Boset Magmatic Segment, GTMS: Gademsa–Tullu Moye Magmatic Segment.

seismic velocity (Fig. 5a), highest Poisson's ratios (Fig. 6), and thick crust relative to the rest of the NMER (Fig. 4c), and we speculate that the magmatic processes that have caused the high Poisson's ratios and high seismic velocity have also locally thickened the crust (with respect to the rest of the NMER) in a zone of overall extension. A cluster of seismicity was observed beneath the FDMS (Fig. 2; Keir et al., 2006) at 8–16 km depth, attesting to the high level of activity in the NMER. Strain is accommodated both in the central magmatic segments and along the border faults.

A clear and abrupt transition in crustal properties is seen from the NMER into the CMER. Based on seismic and gravity data, crustal thickness increases rapidly from 33–35 km in the southernmost NMER to 38–40 km in the CMER (Dugda et al., 2005; Maguire et al., 2006; Mickus et al., 2007; Stuart et al., 2006) (Fig. 3b). The majority of this thickening occurs in the upper crust, which in addition to being thicker has a significantly lower seismic velocity (5.9–6.4 km/s) than the NMER (Maguire et al., 2006). P_n velocity was not measured beneath the CMER, but the EAGLE gravity model along Line 2 requires a higher density (100 kg/m^3) in the uppermost mantle beneath the CMER (Mickus et al., 2007), implying that the P_n velocity is also probably higher by 0.4 km/s (Christensen and Mooney, 1995). From our seismic compilation (Fig. 4b) the locus of crustal thinning in the CMER appears to be near the western rift boundary, although the amount of thinning beneath this margin relative to the adjacent southwestern shoulder is small, ~1–2 km and nearly within the error bars of the measurements (Fig. 4). This small difference in crustal thickness between the rift valley and rift shoulders is in stark contrast to the 5–15 km difference between the NMER and its shoulders and provides evidence that the extensional process in the CMER has been different from the NMER. The highest values of Poisson's ratios in the CMER, 0.33–0.35 (Fig. 6), are near the western boundary beneath the volcanic centers near Butajira and Debre Zeit. Unlike seismicity beneath the magmatic segments in the center of the NMER, seismicity in the CMER is concentrated near the eastern rift boundary (Keir et al., 2006).

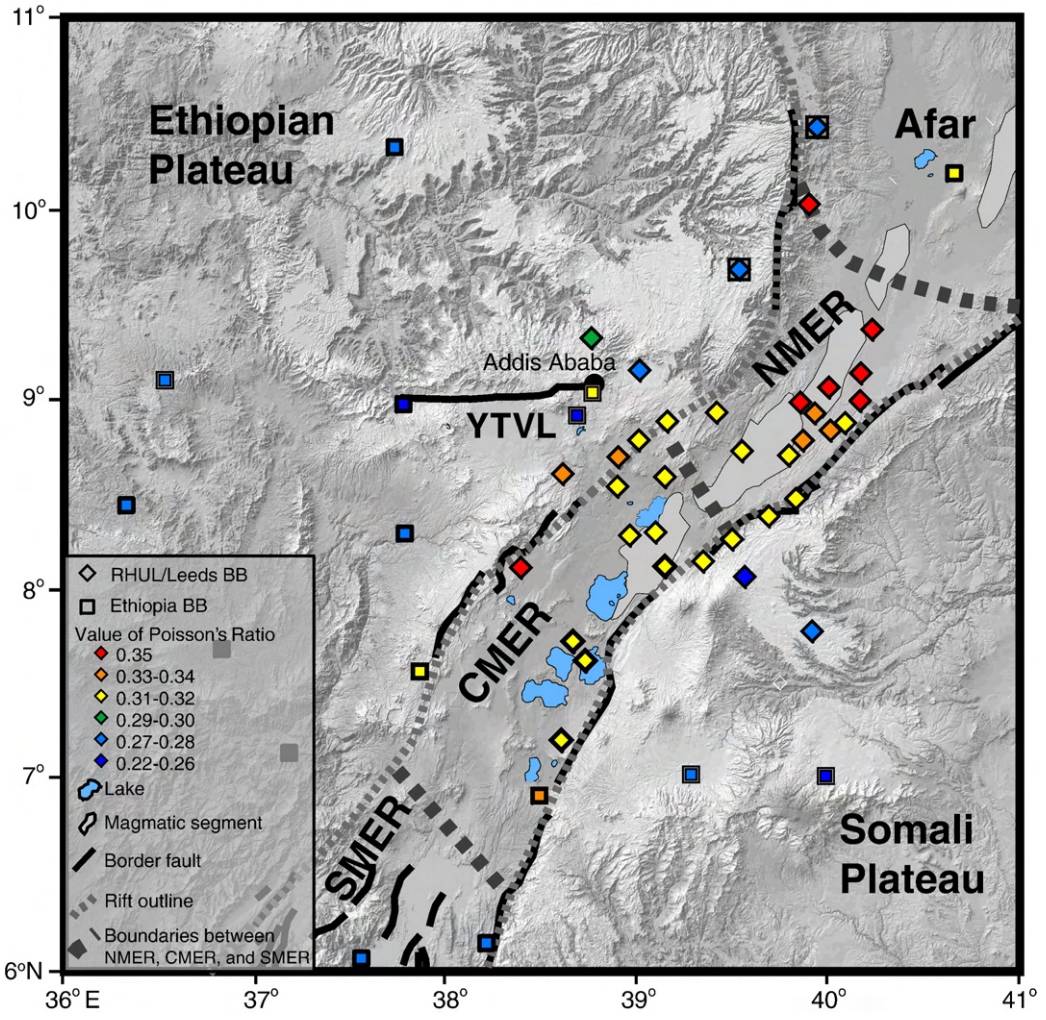

Fig. 6. Values of Poisson's ratio color-coded by magnitude. Red and orange symbols indicate values between 0.33–0.35. These stations are located near the Fentale–Dofen magmatic segment in the NMER, which has experienced historic volcanism, and near the Butajira and Debre Zeit volcanic centers in the CMER. Yellow symbols indicate values from 0.31–0.32. These stations are predominantly within the rift valley, in the NMER and the CMER. Blue and green symbols represent values lower than or equal 0.30, and are located on the rift shoulders.

In contrast to the upper crust, the lower crust is of relatively constant thickness and velocity from the NMER to the CMER. The greater mafic intrusion clearly evident in the upper crust in the NMER (from the refraction velocities, Fig. 3b) has presumably also thickened the lower crust sufficiently to maintain relatively constant lower-crustal thickness along the length of the central and northern MER despite increasing extension in the NMER. This higher degree of magmatism is possibly not visible in the observed seismic velocity (Fig. 3b) because of the expected difference in thermal structure between the two segments.

We interpret the observations in the CMER of thicker crust, lower seismic velocities, and the lack of well-defined surficial magmatic segments to indicate that the CMER is less extended and less magmatically modified than the NMER. The lower seismicity in the CMER appears to indicate that this sector is also currently less active. This abrupt change in rift structure, rift character, volcanic activity and seismicity along the axis of the rift represents a segmentation that continues into the mantle lithosphere. It is observed in upper-mantle tomographic models at 75 km depth (Fig. 4b; Bastow et al., 2005) where an abrupt discontinuity in the mantle slow-velocity anomaly underlies the NMER–CMER transition. The slow velocity anomaly present beneath the NMER is deflected westward beneath the YTVL rather than continuing into the CMER, and a separate upper-

mantle anomaly is present beneath the CMER. This segmentation is also modeled in the along-axis EAGLE gravity model, which shows a step in upper mantle density of 100 kg/m^3 at the NMER–CMER transition (Mickus et al., 2007).

Altogether these observations point to a marked change in crustal and upper mantle structure between the NMER and the CMER. We interpret that the segmentation reflects a discontinuity in the amount of extension and magmatism between the two rift sectors. The thicker crust in the CMER reflects the lower amount of extension, and the lower magnitude upper-crustal velocities in the CMER reflect the lower degree of magmatic addition to the crust.

6.3. Evidence for strain accommodation in the YTVL

The YTVL, an E–W trending zone of extension and magmatism (Fig. 1), is not usually considered part of the Cenozoic MER system. Our compilation of recent data, however, shows that the YTVL has experienced, and still experiences, strain and magmatic intrusion. The YTVL intersects the MER near the boundary between the NMER and the CMER (Fig. 1) at a location along the MER characterized by a monocline as opposed to well-defined border faults. A full analysis of the evolution of the MER needs to include an analysis of the relationship between the MER sectors and the YTVL.

Volcanism in the YTVL and extension along the Ambo fault were coeval with volcanism and extension in the NMER. A cluster of small magnitude earthquakes was recorded along the eastern part of the YTVL during the 2001–2003 EAGLE deployment (Fig. 2; Keir et al., 2006), providing evidence for ongoing strain south and west of Addis Ababa. The regional Bouguer gravity anomaly map (Mickus et al., 2007), bandpassed at wavelengths between 25 and 250 km, and upper-crustal seismic tomography (Fig. 5a) both show a trend in the NMER beneath the magmatic segments which turns to the west towards the YTVL. Based on these gravity and tomography results, we interpret a zone of crustal mafic intrusions to be present off the axis of the rift near the intersection of the NMER and the YTVL (Fig. 5). Magnetotelluric data show evidence for melt in the crust in this region at 20–25 km depth (Whaler and Hautot, 2006), which may be associated with the presence of the YTVL.

The existence of the YTVL, a zone of extension and magmatism along one of the primary pre-rift lithospheric boundaries (between the northwest and southwest shoulders), is important in understanding the propagation of the rift and the role of these pre-rift structures.

7. Interpretation of rift propagation and control by inherited structure

7.1. Rift propagation

The spatial pattern of extension and magmatism in the MER, the presence and characteristics of the YTVL, and the pre-rift lithospheric structure can be combined to develop an interpretation of the evolution of the MER system.

The discontinuity between the NMER and the CMER is critical to understanding the rift's propagation. The discontinuous structure shows that propagation was not a smooth process but rather a process with punctuated episodes of extension and relative quiescence. We propose that rift propagation from north to south began smoothly in the NMER at ~11.5 Ma, as dated by Wolfenden et al., 2004, then stalled upon reaching the NMER–CMER boundary and was diverted around the south margin of the northwest shoulder along the YTVL, which experienced extension and volcanism coeval with the NMER (Abebe et al., 1998) (Fig. 7). Extension eventually focused into a narrow zone in the CMER at about 5–6 Ma (Bonini et al., 2005), largely cutting off extension in the YTVL and connecting the NMER with the SMER in the south. The focusing of extension into the CMER and away from the YTVL may be related to an observed rotation in the stress field between 6.6 Ma and 3.5 Ma from N130°E to N105°E (Wolfenden et al., 2004), which would have made extension along the YTVL less favorable and extension along the CMER more favorable.

Evidence for such a stress field rotation includes both detailed structural and stratigraphic field mapping and kinematic arguments. The NE–SW trending border faults could have formed either orthogonal to an originally NW–SE extension direction, or could have formed along pre-existing weaknesses oblique to a stress field with an E–W oriented extension direction. Detailed stratigraphic and structural analysis in the NMER (Wolfenden et al., 2004) provides compelling evidence for the original NW–SE extension direction. Faults active during the deposition of the Kessem formation (10.6 to 6.6 Ma) strike N35–45E subparallel to the border fault systems and were later superceded by faults striking N15E that were active during and after the deposition of the Balchi formation (3.5 to 2.5 Ma) (Wolfenden et al., 2004). This suggests a change in extension direction during the period of non-deposition between 6.6 and 3.5 Ma.

Additional evidence for such a rotation is provided by kinematic arguments related to seafloor spreading

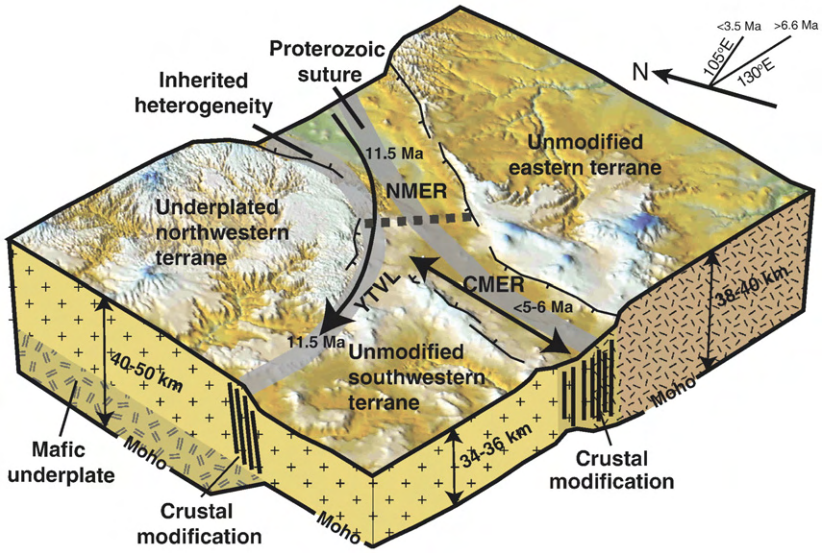

Fig. 7. Lithospheric terranes, crustal thickness, and locations of Cenozoic extension and volcanism (NMER, CMER, YTVL). Cenozoic extension follows the rheological boundaries along the edges of the underplated northwestern block and the boundary between the eastern and western crustal terranes. The location at which rift propagation stalled and was diverted to the west corresponds to the southern edge of the underplated block. The SMER is not included in this diagram because data is limited in this rift sector and on the adjacent shoulders. Compass rose shows extension directions prior to 6.6 Ma (N130°E) and after 3.5 Ma (N105°E) (Wolfenden et al., 2004). The thick dashed gray line shows our redefined CMER–NMER boundary.

and plate motions. The change in extension direction would have occurred during a period of significant changes in plate boundaries and kinematics in the Afar triple junction zone, when seafloor spreading in the Red Sea began at 4 Ma (Kidane et al., 2003). Such a change is also consistent with models of Nubia–Somalia motions deduced from seafloor spreading anomaly patterns (Calais et al., 2003; Lemaux et al., 2002). The change in extension direction may therefore be related to the along-axis propagation of seafloor spreading within the Red Sea and Aden rifts (Wolfenden et al., 2004).

The thick, mafic northwestern block that we identify (Fig. 7) appears to have played a significant role in rift evolution. We speculate that the mafic material underplated to the northwestern crust created a stronger block than the previously thicker, normal velocity crust to the east. After emplacement, the underplate had ~20 M.y. to cool prior to the onset of extension at ~11.5 Ma. The edge of the underplate is a rheologic heterogeneity and extension has localized along its eastern and southern boundaries in the NMER and the YTVL respectively. The location at which rift propagation changed direction appears related to the distribution of this underplate; when the rift reached the southern terminus of the underplate it stalled in a north–south sense and strain was accommodated along the E–W trending YTVL along the southern edge of the block.

There is another significant boundary evident across the MER, a change in thickness from 38–40 km beneath the eastern shoulder to 34–36 km beneath the southwestern shoulder (Fig. 4b). The difference in crustal structure from shoulder to shoulder implies a boundary between two distinct crustal terranes. The CMER is now extending along this boundary. This crustal thickness boundary may provide evidence for the location of the N to NNE trending suture that has been interpreted to run through this region by mapping of ophiolitic fragments (Berhe, 1990; Stern et al., 1990; Vail, 1985), Nd isotopic data (Stern, 1990), and SKS-splitting patterns (Gashawbeza et al., 2004). The boundary may also have been a primary factor in controlling the edge of underplating beneath the NW shoulder in the Oligocene as well as localizing extension in the CMER in the Late Miocene.

7.2. Alternative interpretations

We have attempted alternative models to explain the abrupt crustal thickness change, but these models do not adequately fit the accumulation of data in the two rift sectors. One such alternative interpretation is that the thickness of the CMER was maintained or increased during extension by a greater degree of magmatism. In this scenario, the amount of extension in the NMER and

the CMER is similar, but magmatic inputs to the crust are sufficient in the CMER to maintain thickness while lower magmatic inputs in the NMER would lead to progressively thinned crust. This model predicts greater magmatic modification of the crust (higher seismic velocities and higher Poisson's ratio) in the CMER than in the NMER. Instead the opposite is observed; the NMER has higher crustal velocities (Fig. 3b) and higher values of Poisson's ratio (Fig. 6) than the CMER. A second alternative model is that the crust in the CMER was originally thicker than the NMER so that with equal amounts of extension, the crust in the CMER would remain thicker. This model is harder to negate but appears unlikely. If a mafic underplate had been added prior to extension (related to the high-velocity lower crust underplated beneath the northwestern Ethiopian Plateau) this should still be evident in the along-axis seismic and gravity profiles. No such layer is observed.

7.3. Control of inherited structure on irregular propagation

We conclude that the crustal and upper-mantle segmentation represents a discontinuity in the amount of extension and magmatism between the NMER and the CMER, and that this discontinuity was caused by irregular rift propagation resulting from sharp boundaries in inherited lithospheric structure (Fig. 7). This irregular temporal and spatial process created the strong variations in crustal structure between rift sectors that we observe today and allowed the development of a lateral offset and change in rift orientation between the NMER and the CMER, visible in the surface morphology (Fig. 1). Although we lack significant data in the SMER, we hypothesize that a similar discontinuity in crustal structure and extension may exist at the SMER–CMER boundary. The crustal thinning based on gravity and receiver function estimates and the topographic gradient (Fig. 3) appear to support such a transition, although more data are necessary to verify this hypothesis.

Our interpretation of a pause in north–south rift propagation and the formation of a discontinuity between the rift sectors, based on lithospheric structure, is compatible with available geochronologic data. New data demonstrate that rifting in the CMER started at ~5–6 Ma, i.e. ~5–6 M.y. after initial rifting in the NMER (Bonini et al., 2005). The integration of these new and existing geochronologic data into our model of lithospheric structure allows us to explain both the structural and temporal discontinuities in the MER, and relate the discontinuities to inherited structural heterogeneities. Published geochronologic and conceptually-based models of propagation of the MER (i.e. Bonini et al., 2005; Buck, 2006; Rogers, 2006; Wolfenden et al., 2004) have not recognized the fundamental influences of inherited structure on rift propagation, nor the associated structural discontinuities at locations where rift propagation may have stalled.

8. Conclusions

Pre-existing structures have controlled the location and the initial stages of rifting in the Main Ethiopian Rift. Two distinct Proterozoic basement terranes, one strongly underplated beneath its northern part, created rheological boundaries that localized extension and permitted the MER to propagate. Southward propagation in the NMER along the eastern limit of mafic underplating (controlled by the Proterozoic terrane boundary) stalled for 5–6 M.y. at what would become the NMER–CMER boundary, south of which the strong rheological heterogeneity provided by the underplated block was no longer available. The CMER formed along the remainder of the suture only after the rotation of the principal stress direction made extension along the YTVL unfavorable and extension along the CMER more favorable. Our data are focused on the NMER and the CMER, and additional data are required to understand the three-dimensional crustal and lithospheric structure and the role of the inherited structures in controlling the evolution of the SMER.

An important controversy in East African tectonics concerns whether one or two separate mantle plumes are required to explain the temporal and spatial distribution of Tertiary basaltic magmatism (Rogers, 2006). The wide compositional range of African Rift basalts can best be explained with two plume sources, one with high-μ Sr–Nd–Pb–He isotopic affinities, observed south of the Turkana Depression; and one with isotopic signatures analogous to those observed in some ocean islands, present throughout the Ethiopian Rift and the Afar region (Furman, 2007). Rogers' major perceived impediment to the 'two-plume' model is the concept of a simple northward propagation of magmatism and rifting from southern Ethiopia towards Afar (Wolfenden et al., 2004) that is in the opposite direction to that predicted by the northward motion of Africa (O'Connor et al., 1999) over a stationary hot spot (Rogers, 2006). Our more complex model of discontinuous rifting, including southward rift propagation from the NMER into the CMER, therefore removes a previous inconsistency with the 'two-plume' model.

It is evident from observations of upper-mantle upwellings, mafic intrusions in the upper crust, and

surface geology that magmatism plays a major role in the present-day extensional process. Initial formation of the rift, however, by an active tabular magmatic upwelling (as imaged by upper mantle tomography beneath the MER) might imply a synchronous formation of the entire MER above the upwelling. Instead, the formation of the MER has been discontinuous and diachronous, suggesting a process of irregular rift propagation. We here combine geophysical data which show the CMER to be anomalous in crustal thickness and composition with geochronologic data which suggest that the CMER is younger than either the SMER or the NMER by 5–6 M.y. Our model of irregular propagation suggests that magmatic control of rifting in the MER is a secondary phase of rift evolution rather than the primary phase. Initial rifting, whether driven by broader mantle upwellings, plate boundary forces, or most likely a combination of the two, initiated along inherited weaknesses in the continental lithosphere. The present mantle upwellings and magmatic processes that now control rift evolution were organized by initial rift structures into the along-axis segmented pattern that is observable today. If the MER, which seems so dominated by magmatic processes, was in its early evolution controlled by lithospheric structure, lithospheric structure seems likely to have been equally or more important in the evolution of similarly or less magmatic rifts worldwide.

Acknowledgements

EAGLE data acquisition was funded by National Science Foundation (NSF) Continental Dynamics grant EAR0208475 and the Natural Environment Research Council. We appreciate the continued willingness of Ethiopian scientists to host and collaborate with US geophysicists. We thank Andy Nyblade, Nicky White, and an anonymous reviewer for their thoughtful reviews.

References

Abebe, T., Mazzarini, F., Innocenti, F., Manetti, P., 1998. The Yerer–Tullu Wellel Volcanotectonic lineament: a transtensional structure in central Ethiopia and the associated magmatic activity. J. Afr. Earth Sci. 26, 135–150.

Abebe, T., Manetti, P., Bonini, M., Corti, G., Innocenti, F., and Mazzarini, F., 2005, Geological map (scale 1:200,000) of the northern Main Ethiopian Rift and its implication for the volcano-tectonic evolution of the rift, Geol. Soc. Am. Map Chart Ser., MCH094.

Abebe, B., Acocella, V., Korme, T., Ayalew, D., 2007. Quaternary faulting and volcanism in the Main Ethiopian Rift. J. Afr. Earth Sci. 48, 115–124.

Baker, J., Snee, L., Menzies, M., 1996. A brief Oligocene period of flood volcanism in Yemen. Earth Planet. Sci. Lett. 138, 39–55.

Bastow, I.D., Stuart, G.W., Kendall, J.-M., Ebinger, C.J., 2005. Upper-mantle seismic structure in a region of incipient continental breakup: northern Ethiopian rift. Geophys. J. Int. 162, 479–493.

Bendick, R., McClusky, S., Bilham, R., Asfaw, L., Klemperer, S., 2006. Distributed Nubia–Somalia relative motion and dike intrusion in the Main Ethiopian Rift. Geophys. J. Int. 165, 303–310.

Benoit, M.H., Nyblade, A.A., VanDecar, J.C., 2006. Upper mantle P-wave speed variations beneath Ethiopia and the origin of the Afar hotspot. Geology 34, 329–332.

Berckhemer, H., Baier, B., Bartelson, H., Behle, A., Burkhardt, H., Gebrande, H., Makris, J., Menzel, H., Miller, H., Vees, R., 1975. Deep seismic soundings in the Afar region and on the highland of Ethiopia. In: Pilger, A., Rosler, A. (Eds.), Afar Depression of Ethiopia, vol. I. Schweizerbart, Stuttgart, pp. 89–107.

Berhe, S.M., 1990. Ophiolites in northeast and East Africa: implications for Proterozoic crustal growth. J. Geol. Soc. (Lond.) 147, 41–57.

Bonini, M., Corti, G., Innocenti, F., Manetti, P., Mazzarini, F., Abebe, T., Pecskay, Z., 2005. Evolution of the Main Ethiopian Rift in the frame of Afar and Kenya rifts propagation. Tectonics 24, TC1007. doi:10.1029/2004TC001680.

Buck, W.R., 2006. The role of magma in the development of the Afro-Arabian Rift System. In: Yirgu, G., Ebinger, C.J., Maguire, P.K.H. (Eds.), The Afar Volcanic Province within the East African Rift System. Geol. Soc. Spec. Publ., vol. 259, pp. 43–54.

Burke, K., Sengor, A.M.C., 1986. Tectonic escape in the evolution of the continental crust. In: Barazangi, M., Brown, L. (Eds.), Reflection Seismology: The Continental Crust. Geodyn. Ser., vol.14. AGU, Washington, D. C., pp. 41–53.

Calais, E., DeMets, C., Nocquet, J.-M., 2003. Evidence for post-3.16 Ma change in Nubia–Eurasia–North America plate motions. Earth Planet. Sci. Lett. 216, 81–92.

Chernet, T., Hart, W., Aronson, J., Walter, R.C., 1998. New age constraints on the timing of volcanism and tectonism in the northern Main Ethiopian Rift — southern Afar transition zone (Ethiopia). J. Volcanol. Geotherm. Res. 80, 267–280.

Christensen, M.I., Mooney, W.D., 1995. Seismic velocity structure and composition of the continental crust — a global view. J. Geophys. Res. 100, 9761–9788.

Church, W.R., 1991. Discussion of "Ophiolites in northeast and East Africa: implications for Proterozoic crustal growth". J. Geol. Soc. (Lond.) 48, 600–606.

Cornwell, D.G., Mackenzie, G.D., England, R.W., Maguire, P.K.H., Asfaw, L.M., Oluma, B., 2006. Northern Main Ethiopian Rift crustal structure from new high-precision gravity data. In: Yirgu, G., Ebinger, C.J., Maguire, P.K.H. (Eds.), The Afar Volcanic Province within the East African Rift System. Geol. Soc. Spec. Publ., vol. 259, pp. 307–321.

Courtillot, V., 1982. Propagating rifts and continental breakup. Tectonics 1, 239–250.

Courtillot, V., Vink, G.E., 1983. How continents break up. Sci. Am. 249, 42–49.

Dugda, M.T., Nyblade, A.A., Julia, J., Langston, C.A., Ammon, C.J., Simiyu, S., 2005. Crustal structure in Ethiopia and Kenya from receiver function analysis: implications for rift development in eastern Africa. J. Geophys. Res. 110, B01303. doi:10.1029/2004JB003065.

Dunbar, J.A., Sawyer, D.S., 1988. Continental rifting at pre-existing lithospheric weaknesses. Nature 333, 451–452.

Dunbar, J.A., Sawyer, D.S., 1989. Patterns of continental extension along the conjugate margins of the central and north Atlantic Oceans and Labrador Sea. Tectonics 8, 1059–1077.

Dunbar, J.A., Sawyer, D.S., 1996. Three-dimensional dynamic model of continental rift propagation and margin plateau formation. J. Geophys. Res. 101, 27845–27863.

Ebinger, C.J., Yemane, T., WoldeGabriel, G., Aronson, J.L., Walter, R.C., 1993. Late Eocene — recent volcanism and faulting in the southern main Ethiopian rift. J. Geol. Soc. (Lond.) 150, 99–108.

Ebinger, C.J., Hayward, N., 1996. Soft plates and hot spots: constraints from the Ethiopian and Afar rifts. J. Geophys. Res. 101, 21859–21876.

Ebinger, C.J., Sleep, N.H., 1998. Cenozoic magmatism throughout east Africa resulting from impact of a single plume. Nature 395, 788–791.

Ebinger, C., Yemane, T., Harding, D., Tesfaye, S., Rex, D., Kelley, S., 2000. Rift deflection, migration, and propagation: linkage of the Ethiopian and Eastern rifts, Africa. Geol. Soc. Amer. Bull. 102, 163–176.

Endeshaw, A., 1988. Current status (1987) of geothermal exploration in Ethiopia. Geothermics 17, 477–488.

Furman, T., Bryce, J., Rooney, T., Hanan, B., Yirgu, G., Ayalew, D., 2006. Heads and tails: 30 million years of the Afar plume. In: Yirgu, G., Ebinger, C.J., Maguire, P.K.H. (Eds.), The Afar Volcanic Province within the East African Rift System, SP259. Geol. Soc. Spec. Publ., pp. 95–119.

Furman, T., 2007. Geochemistry of East African Rift basalts: an overview. J. Afr. Earth Sci. 48, 147–160.

Gashawbeza, E.M., Klemperer, S.L., Nyblade, A.A., Walker, K.T., Keranen, K.M., 2004. Shear-wave splitting in Ethiopia: precambrian mantle anisotropy locally modified by Neogene rifting. Geophys. Res. Lett. 31, L18602. doi:10.1029/2004GL020471.

George, R., Rogers, N., 2002. Plume dynamics beneath the African plate inferred from the geochemistry of the Tertiary basalts of southern Ethiopia. Contrib. Mineral. Petrol. 144, 286–304.

Gibson, I.L., 1969. The structure and volcanic geology of an axial portion of the Main Ethiopian Rift. Tectonophysics 8, 561–565.

Hill, R.I., 1991. Starting plumes and continental break-up. Earth Planet. Sci. Lett. 104, 398–416.

Hofmann, C., Courtillot, V., Feraud, G., Rochette, P., Yirgu, G., Ketefo, E., Pik, R., 1997. Timing of the Ethiopian flood basalt event: implications for plume birth and global change. Nature 389, 838–841.

Keir, D., Ebinger, C.J., Stuart, G.W., Daly, E., Ayele, A., 2006. Strain accommodation by magmatism and faulting as rifting proceeds to breakup: seismicity of the northern Ethiopian rift. J. Geophys. Res. 111, B05314. doi:10.1029/2005JB003748.

Kendall, J.-M., Pilidou, S., Keir, D., Bastow, I.D., Stuart, G.W., Ayele, A., 2006. Mantle upwellings, melt migration, and the rifting of Africa: insights from seismic anisotropy. In: Yirgu, G., Ebinger, C.J., Maguire, P.K.H. (Eds.), The Afar Volcanic Province within the East African Rift System, SP259. Geol. Soc. Spec. Publ., pp. 55–72.

Keranen, K., Klemperer, S., Gloaguen, R., and the EAGLE Working Group, 2004. Three-dimensional seismic imaging of a protoridge axis in the main Ethiopian rift. Geology 32, 949–952.

Kidane, T., Courtillot, V., Manighetti, I., Audin, L., Lahitte, P., Quidelleur, X., Gillot, P.-Y., Gallet, Y., Carlut, J., Haile, T., 2003. New paleomagnetic and geochronologic results from Ethiopian Afar: block rotations linked to rift overlap and propagation and determination of a similar to 2 Ma reference pole for stable Africa. J. Geophys. Res 108, 2102–2122.

Lemaux, J., Gordon, R.G., Royer, J.-Y., 2002. Location of the Nubia–Somalia boundary along the Southwest Indian Ridge. Geology 30, 339–342.

Mackenzie, G.D., Thybo, H., Maguire, P.K.H., 2005. Crustal velocity structure across the main Ethiopian Rift; results from two-dimensional wide-angle seismic modelling. Geophys. J. Int. 162, 994–1006.

Maguire, P.K.H., Ebinger, C.J., Stuart, G.W., Mackenzie, G.D., Whaler, K.A., Kendall, J.-M., Khan, M.A., Fowler, C.M.R., Klemperer, S.L., Keller, G.R., Harder, S., Furman, T., Mickus, K., Asfaw, L., Ayele, A., Abebe, B., 2003. Geophysical project in Ethiopia studies continental breakup. EOS Trans. AGU. 84 (337), 342–343.

Maguire, P.K.H., Keller, G.R., Klemperer, S.L., MacKenzie, G.D., Keranen, K., Harder, S., O'Reilly, B., Thybo, H., Asfaw, L., Khan, M.A., Amha, M., 2006. Crustal structure of the northern Main Ethiopian Rift from the EAGLE controlled-source survey; a snapshot of incipient lithospheric break-up. In: Yirgu, G., Ebinger, C.J., Maguire, P.K.H. (Eds.), The Afar Volcanic Province within the East African Rift System, SP259. Geol. Soc. Spec. Publ., pp. 269–292.

Mahatsente, R., Jenztsch, G., Jahr, T., 1999. Crustal structure of the Main Ethiopian Rift from gravity data: 3-D modelling. Tectonophysics 313, 363–382.

Mickus, K., Tadesse, K., Keller, G., Oluma, B., 2007. Gravity analysis of the Main Ethiopian Rift. J. Afr. Earth Sci. 48, 59–69.

Montelli, R., Nolet, G., Dahlen, F.A., Masters, G., 2006. A catalogue of deep mantle plumes: new results from finite frequency tomography. Geochem. Geophys. Geosyst. 7, Q11007. doi:10.1029/2006GC001248.

Nyblade, A.A., Langston, C.A., 2002. Broadband seismic experiments probe the East African rift. EOS Trans. AGU 83, 405–408.

Nyblade, A.A., Brazier, R.A., 2002. Precambrian lithospheric controls on the development of the East African Rift System. Geology 30, 755–758.

O'Connor, J.M., Stoffers, P., van den Bogaard, P., McWilliams, M., 1999. First seamount age evidence for significantly slower African plate motion since 19 to 30 Ma. Earth Planet. Sci. Lett. 171, 575–589.

Pascal, C., van Wijk, J.W., Cloetingh, S.A.P.L., Davies, G.R., 2002. Effect of lithosphere thickness heterogeneities in controlling rift localization: numerical modeling of the Oslo Graben. Geophys. Res. Lett. 29, 1355. doi:10.1029/2001GL014354.

Pizzi, A., Coltori, M., Abebe, B., Disperati, L., Sacchi, G., Salvini, R., 2006. The Wonji fault belt (Main Ethiopian Rift): structural and geomorphological constraints and GPS monitoring. In: Yirgu, G., Ebinger, C.J., Maguire, P.K.H. (Eds.), The Afar Volcanic Province within the East African Rift System, SP259. Geol. Soc. Spec. Publ., pp. 191–207.

Rogers, N.W., 2006. Basaltic magmatism and the geodynamics of the East African Rift System. In: Yirgu, G., Ebinger, C.J., Maguire, P.K.H. (Eds.), The Afar Volcanic Province within the East African Rift System, SP259. Geol. Soc. Spec. Publ., pp. 77–93.

Rooney, T.O., Furman, T., Yirgu, G., Ayalew, D., 2005. Structure of the Ethiopian lithosphere: Xenolith evidence in the Main Ethiopian Rift. Geochim. Cosmochim. Acta 69, 3889–3910.

Rooney, T., Furman, T., Bastow, I., Ayalew, D., Yirgu, G., 2007. Lithospheric modification during crustal extension in the Main Ethiopian Rift. J. Geophys. Res. 112, B10201. doi:10.1029/2006JB004916.

Sawyer, D.S., 1985. Total tectonics subsidence, a parameter for distinguishing crust type at the U.S. Atlantic continental margin. J. Geophys. Res. 90, 7751–7769.

Shackleton, R.M., 1986. Precambrian collision tectonics in Africa. In: Coward, M.P., Reis, A.C. (Eds.), Collision Tectonics, SP19. Geol. Soc. Spec. Publ., pp. 329–349.

Stern, R.J., 2002. Crustal evolution in the East African Orogen: a neodymium isotopic perspective. J. Afr. Earth Sci. 34, 109–117.

Stern, R.J., Nielsen, K.C., Best, E., Sultan, M., Arvidson, R.E., Kroner, A., 1990. Orientation of the late Precambrian sutures in the Arabian–Nubian Shield. Geology 18, 1103–1106.

Stuart, G.W., Bastow, I.D., Ebinger, C.J., 2006. Crustal Structure of the northern Main Ethiopian Rift from receiver function studies. In:

Yirgu, G., Ebinger, C.J., Maguire, P.K.H. (Eds.), The Afar Volcanic Province within the East African Rift System, SP259. Geol. Soc. Spec. Publ., pp. 253–267.

Tiberi, C., Ebinger, C., Ballu, V., Stuart, G., Oluma, B., 2005. Inverse models of gravity data from the Red Sea–Aden–East African rifts triple junction zone. Geophys. J. Int. 163, 775–787.

Tommasi, A., Vauchez, A., 2001. Continental rifting parallel to ancient collisional belts: an effect of the mechanical anisotropy of the lithospheric mantle. Earth Planet. Sci. Lett. 185, 199–210.

Ukstins, I., Renne, P., Wolfenden, E., Baker, J., Menzies, M., 2002. Matching conjugate volcanic rifted margins: $^{40}Ar/^{39}Ar$ chronostratigraphy of pre- and syn-rift bimodal flood volcanism in Ethiopia and Yemen. Earth Planet. Sci. Lett. 198, 289–306.

Vail, J.R., 1985. Pan-African (late Precambrian) tectonic terrains and the reconstruction of the Arabian-Nubian Shield. Geology 13, 839–849.

van Wijk, J.W., 2005. Role of weak zone orientation in continental lithosphere orientation. Geophys. Res. Lett. 32, L02303. doi:10.1029/2004GL022192.

van Wijk, J.W., Blackman, D.K., 2005. Dynamics of continental rift propagation: the end-member modes. Earth and Planet. Sci. Lett. 229, 247–258.

Vauchez, A., Barruol, G., Tommasi, A., 1997. Why do continents breakup parallel to ancient orogenic belts? Terra Nova 9, 62–66.

Vauchez, A., Tommasi, A., Barrruol, G., 1998. Rheological heterogeneity, mechanical anisotropy and deformation of the continental lithosphere. Tectonophysics 296, 61–86.

Whaler, K.A., Hautot, S., 2006. The electrical resistivity structure of the crust beneath the northern Main Ethiopian Rift. In: Yirgu, G., Ebinger, C.J., Maguire, P.K.H. (Eds.), The Afar Volcanic Province within the East African Rift System, SP259. Geol. Soc. Spec. Publ., pp. 293–305.

WoldeGabriel, G., Aronson, J., Walter, R., 1990. Geology, geochronology, and rift basin development in the central sector of the Main Ethiopian rift. Geol. Soc. Am. Bull. 102, 439–458.

WoldeGabriel, G., Yemane, T., White, T., Asfaw, B., Suwa, G., 1991. Age of volcanism and fossils in the Burji–Soyoma area, Amaro Horst, southern Main Ethiopian Rift. J. Afr. Earth Sci. 13, 437–447.

Wolfenden, E., Ebinger, C., Yirgu, G., Deino, A., Ayalew, D., 2004. Evolution of the northern Main Ethiopian rift: birth of a triple junction. Earth Planet. Sci. Lett. 224, 213–228.